A T6SS in the coral pathogen *Vibrio coralliilyticus* secretes an arsenal of anti-eukaryotic effectors and contributes to virulence

Short title:

***Vibrio coralliilyticus* T6SS effector repertoires**

Shir Mass[1], Hadar Cohen[1], Motti Gerlic[1], Blake Ushijima[2], Julia C. van Kessel[3], Eran Bosis[4], and Dor Salomon[1,*]

[1] Department of Clinical Microbiology and Immunology, School of Medicine, Faculty of Medical and Health Sciences, Tel Aviv University, Israel

[2] Department of Biology and Marine Biology, University of North Carolina Wilmington, Wilmington, NC, USA

[3] Department of Biology, Indiana University, Bloomington, Indiana, USA

[4] Department of Biotechnology Engineering, Braude College of Engineering, Karmiel, Israel

[*] For correspondence: dorsalomon@mail.tau.ac.il

Keywords: T6SS, *Vibrio coralliilyticus*, *Artemia*, competition, virulence, effectors

Abstract

Vibrio coralliilyticus (*Vcor*) is a pathogen of coral and shellfish, leading to devastating economic and ecological consequences worldwide. Although rising ocean temperatures correlate with increased *Vcor* pathogenicity, the specific molecular mechanisms and determinants contributing to virulence remain poorly understood. Here, we systematically analyzed the type VI secretion system (T6SS), a contact-dependent toxin delivery apparatus, in *Vcor*. We identified two omnipresent T6SSs that are activated at temperatures in which *Vcor* becomes virulent; T6SS1 is an antibacterial system mediating interbacterial competition, whereas T6SS2 mediates anti-eukaryotic toxicity and contributes to mortality during infection of an aquatic model organism, *Artemia salina*. Using comparative proteomics, we identified the T6SS1 and T6SS2 toxin arsenals of three *Vcor* strains with distinct disease etiologies. Remarkably, T6SS2 secretes at least nine novel anti-eukaryotic toxins comprising core and accessory repertoires. We propose that T6SSs differently contribute to *Vcor*'s virulence: T6SS2 plays a direct role by targeting the host, while T6SS1 plays an indirect role by eliminating competitors.

Author Summary

Coral reefs are diverse ecosystems providing habitats for various fish, invertebrates, and microorganisms. Climate change, leading to rising ocean water temperatures, correlates with coral bleaching and mass mortality events. An implicated causal agent of coral disease outbreaks is the marine bacterium *Vibrio coralliilyticus*. Here, we found that two toxin injection systems present in all *Vibrio coralliilyticus* strains are regulated by temperature; we revealed the toxins that they secrete and their function in competition against rival bacteria and in the intoxication of an animal host. Our findings implicate these systems as previously unappreciated contributors to *Vibrio coralliilyticus* virulence, illuminating possible targets to treat or prevent coral infection.

Introduction

The oceans are home to Gram-negative marine bacteria of the genus *Vibrio*. These include many established and emerging pathogens that infect humans and marine animals [1,2]. In the past, vibrios were primarily associated with the warmer equatorial waters. Yet, in recent decades, they have spread to other regions, including the northern USA, Canada, and North Europe [3,4]. This spread correlates with rising ocean surface-level temperatures and disease outbreaks [5,6].

Corals are marine animals affected by rising ocean temperatures caused by climate change and the spread of vibrios [7–9]. They are ecologically and economically important because they provide diverse ecosystems used as habitats for various fish and invertebrates, as well as helping to protect shorelines from storm surges and erosion [10]. The coral animal lives in a symbiotic relationship with photosynthetic endosymbiotic dinoflagellates and microbes (collectively called the coral holobiont) [11–14]. *Vibrio coralliilyticus* (*Vcor*) is a bacterial pathogen shown to be a cause of diseases resulting in bleaching or tissue loss in corals [9,15,16]. Among other coral pathogens [9], *Vcor* stands out due to its wide geographic spread and broad range of reported hosts. Aside from corals, *Vcor* is also responsible for mortalities in shellfish hatcheries [17].

The coral holobiont is affected by various environmental conditions, such as shifts in water temperature, pH, and nutrients. Elevated temperature is a key factor in many *Vcor* infections because it increases the abundance and virulence of many *Vcor* strains [14]. At temperatures below 23°C, *Vcor* strains are predominantly not pathogenic [8]. However, the virulence of many strains increases when temperatures rise above 23°C [14,15,18]. In some cases, the symbiotic dinoflagellates are killed, and coral bleaching occurs. With most pathogenic strains, shifts to >27°C result in coral tissue lysis and increased coral mortality [15]. Elevated temperatures are associated with the production of proteases and hemolysins, motility, antimicrobial resistance, and secretion systems in *Vcor* [19]. In addition, the expression of *toxR*, a transcription regulator associated with virulence in other vibrios [20], correlates with increased temperature and was shown to contribute to *Vcor* virulence [21]. These data provide strong evidence that temperature regulates virulence-associated genes in *Vcor.* Nevertheless, it remains unclear how these factors contribute to pathogenicity and whether the same factors play a role in virulence towards different hosts.

Many vibrios employ a specialized toxin delivery mechanism, the type VI secretion system (T6SS), to manipulate their environment [22–29]. The T6SS is a proteinaceous apparatus that is assembled inside the bacterial cell: a sheath structure engulfs an inner tube made of stacked hexameric rings of Hcp proteins, which is capped by a spike comprising a VgrG trimer sharpened by a PAAR repeat-containing protein (hereafter referred to as PAAR) [30]. This tube-spike complex is decorated with toxic proteins, called effectors, that mediate the toxic activities of the T6SS [31–33]. Contraction of the sheath propels the tube-spike complex out of the cell, providing it with sufficient force to penetrate the membrane of a neighboring cell where effectors are deployed [34]. Whereas most T6SSs investigated to date mediate interbacterial competitions by delivering antibacterial effectors, a few T6SSs have been shown to target eukaryotes and mediate virulence [33,35,36]. In accordance, although most *Vibrio* T6SSs play a role in interbacterial competitions [24–28,37–39], we and others recently revealed *Vibrio* T6SSs and effectors that target eukaryotes, and we postulated that they play a role in virulence [22,40–43].

Several studies reported the temperature-dependent expression of T6SS components in *Vcor* [19,42], suggesting that T6SSs play a role in the temperature-regulated transition to a pathogenic lifestyle. The antibacterial activity of one T6SS was previously demonstrated in two

Vcor strains [42,44]. However, the presence of other T6SSs in the *Vcor* pan-genome, their role, regulation, effector repertoire, and contribution to virulence remain unknown. Here, we systematically analyzed the T6SSs in the *Vcor* pan-genome and revealed two omnipresent systems. Using three *Vcor* strains as model systems, we experimentally defined the environmental conditions regulating the activation of these two T6SSs. We also identified their function and effector repertoires. Importantly, we revealed nine novel anti-eukaryotic effectors delivered by the *Vcor* T6SS2, contributing to *Vcor* virulence.

Results

Two T6SSs are omnipresent in Vibrio coralliilyticus strains

To identify the T6SSs found in the pan-genome of *Vibrio coralliilyticus* (*Vcor*), we retrieved the sequences of the core T6SS sheath component, TssB, from 31 available RefSeq *Vcor* genomes (**Dataset S1**) and analyzed their genomic neighborhoods. Our analyses revealed that all genomes harbor two conserved T6SSs, named T6SS1 and T6SS2 (**Fig. 1** and **Dataset S2**), suggesting that these T6SSs play an important role in the *Vcor* lifestyle. T6SS1 is similar to the previously investigated T6SS1 from *V. parahaemolyticus* [24,45], *V. alginolyticus* [26], and *V. proteolyticus* [28], sharing the same gene content and organization. We recently showed that this system mediates interbacterial competition in the *Vcor* type strain BAA-450 and in strain OCN008 [42,44]. Two additional T6SSs, which we named T6SS3 and T6SS4, are each found in a single *Vcor* genome (**Dataset S2**). Notably, two genes encoding structural core components in T6SS4 appear to include frameshifts, and the gene cluster lacks a gene encoding the conserved T6SS core component, TssH (**Fig. 1**). Therefore, it is possible that T6SS4 is not functional.

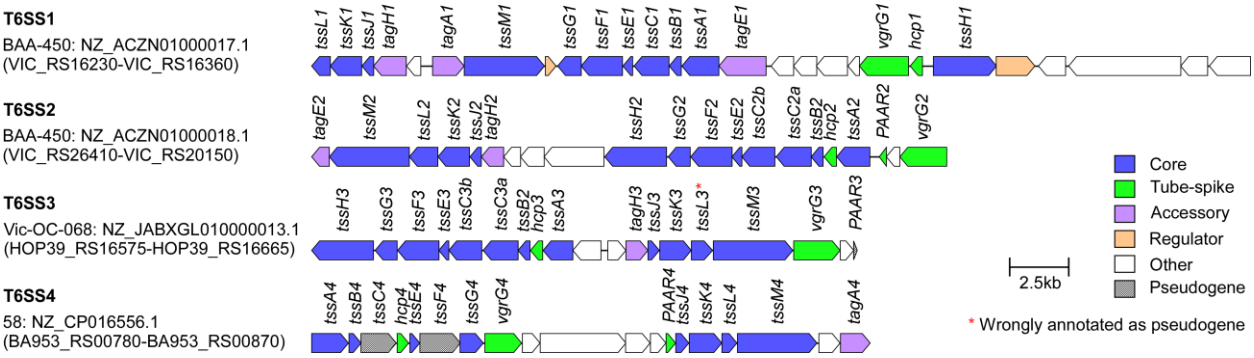

Fig. 1. Representative T6SS gene clusters found in *Vibrio coralliilyticus* genomes. The strain name, GenBank accession number, and the first and last locus tag are denoted on the left. Genes are denoted by arrows indicating the predicted direction of transcription. Encoded proteins or domains are denoted above the genes.

Environmental conditions regulate Vibrio coralliilyticus T6SSs

Because T6SS1 and T6SS2 are omnipresent in *Vcor*, we set out to investigate their activation and function. First, we sought to determine whether T6SS1 and T6SS2 are regulated by environmental conditions regulating *Vcor* virulence. To this end, we selected three representative *Vcor* strains harboring both T6SSs: BAA-450 (the type strain), OCN008, and OCN014. These strains were isolated from different coral hosts and display different disease etiologies [16,46,47]. Strains BAA-450 and OCN014 have a temperature-dependent infection

mode, and they become more virulent as temperatures rise above 23°C; the virulence of strain OCN008 does not significantly change from 23 - 27°C [16,18,21].

To determine whether the activation of T6SS1 and T6SS2 depends on temperature or nutrient availability, we monitored the expression and secretion of the conserved secreted T6SS structural components, VgrG1 and Hcp2 [23], respectively. Bacteria were grown in either rich (marine LB; MLB) or poor (glycerol artificial sea water; GASW) media and under a range of physiologically relevant temperatures that affect *Vcor* pathogenicity: 19, 23, 28, and 31°C [16,21,46]. As shown in **Fig. 2A-B**, we found that the activity of both T6SS1 and T6SS2 is temperature- and media-dependent. In rich media, both systems are active between 23-31°C; T6SS1 secretion peaks at 28°C, whereas T6SS2 secretion peaks at 31°C (**Fig. 2A**). Notably, secretion via T6SS1 in strain OCN008 appears lower than in BAA-450 and OCN014. In poor media, T6SS1 secretion peaks at 23°C in all strains and is retained at higher temperatures only in strain BAA-450 (**Fig. 2B**); T6SS2 secretion is only observed in strain BAA-450 at 23°C. Comparison between the activity of both systems in rich and poor media at 28°C revealed higher levels of secretion in rich media (**Fig. 2C**). Therefore, unless otherwise indicated, we performed subsequent analyses of T6SS1 and T6SS2 when *Vcor* strains are grown in rich media at 28°C, conditions in which both systems are active in all three strains.

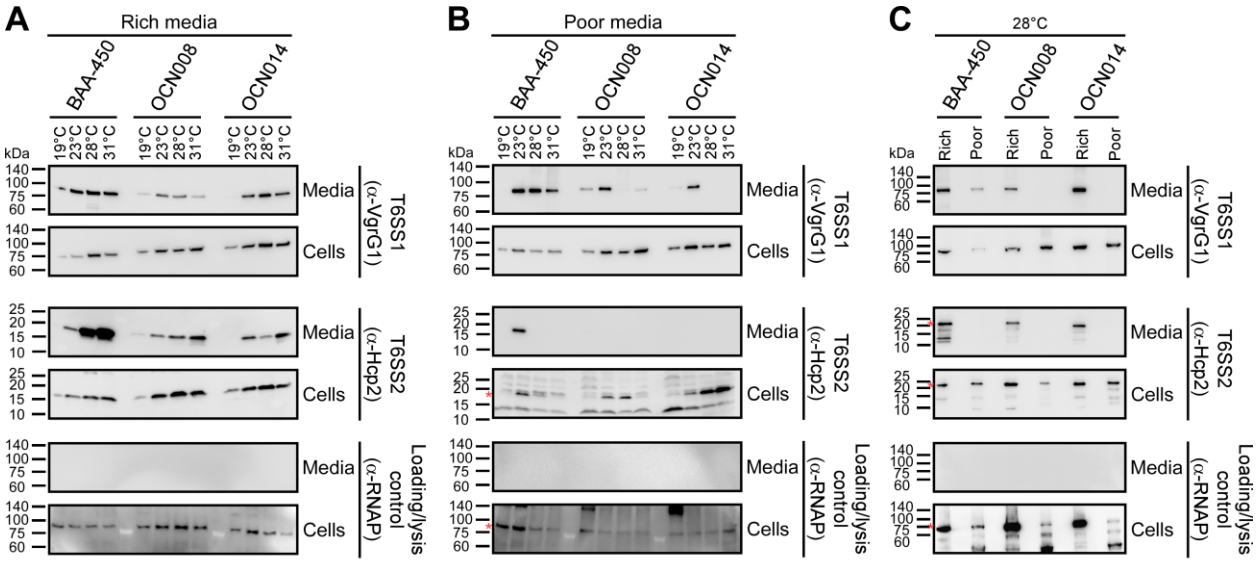

Fig. 2. *Vibrio coralliilyticus* T6SS1 and T6SS2 are regulated by environmental conditions. Expression (cells) and secretion (media) of VgrG1 and Hcp2 from the three indicated *Vcor* strains grown for 4 hours at the indicated temperatures in "rich" marine LB medium **(A)** or "poor" glycerol artificial sea water medium **(B)**. **C)** Comparison of VgrG1 and Hcp2 expression and secretion when *Vcor* strains were grown at 28°C in "rich" or "poor" media. RNA polymerase sigma 70 (RNAp) was used as a loading and lysis control. Asterisks denote expected protein sizes. Results from a representative experiment out of at least three independent experiments are shown.

T6SS1 mediates interbacterial competitions

We previously reported that T6SS1 in strains BAA-450 and OCN008 mediates antibacterial activity during interbacterial competitions [42,44]. To determine whether this is also true for T6SS1 in strain OCN014 and whether T6SS2 also plays a role in interbacterial competition, we

set out to monitor the outcome of interbacterial competitions using *Vcor* strains in which the two T6SSs were inactivated, either individually or together. To this end, we first constructed *Vcor* mutant strains in which we inactivated T6SS1 by deleting the gene encoding the conserved structural component Hcp1 (Δ*hcp1*), and T6SS2 by deleting the gene encoding the conserved structural component TssM2 (Δ*tssM2*) (**Fig. S1A**). These mutations did not affect bacterial growth (**Fig. S1B**). When competed against a sensitive a *V. natriegens* prey strain on rich media plates at 28°C, all three *Vcor* strains killed the prey, evident by the decrease in prey viability during the four hours of co-incubation with the wild-type *Vcor* attackers (**Fig. 3A-C**). This killing was dependent on T6SS1, since its inactivation in the attacker strains by deleting *hcp1* abolished the toxicity. Inactivation of T6SS2 by deleting *tssM2*, either alone or in combination with an inactive T6SS1, had no effect on the observed antibacterial activity of *Vcor*. Taken together, our results confirm that the *Vcor* T6SS1 mediates antibacterial activity and suggest that T6SS2 does not play a role in interbacterial competition.

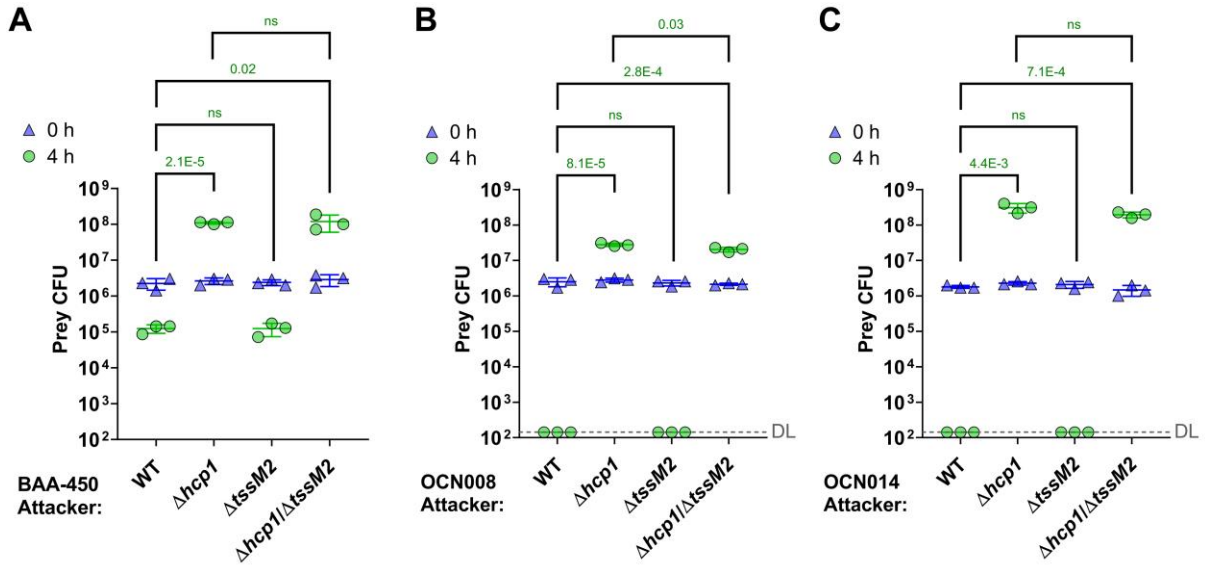

Fig. 3. *Vibrio coralliilyticus* T6SS1 mediates interbacterial competition. A-C) Viability counts (colony forming units; CFU) of *V. natriegens* prey strains before (0 h) and after (4 h) co-incubation with the indicated *Vcor* BAA-450 (A), OCN008 (B), or OCN014 (C) attacker strains on MLB plates at 28°C. The statistical significance between samples at the 4 h time point was calculated using an unpaired, two-tailed Student's *t* test; ns, no significant difference ($P > 0.05$); WT, wild-type; DL, the assay's detection limit. Data are shown as the mean ± SD; $n = 3$. The data shown are a representative experiment out of at least three independent experiments.

T6SS2 targets eukaryotes

Based on the above results, we hypothesized that T6SS2 mediates anti-eukaryotic activities. To investigate whether T6SS2 plays a role in bacterial virulence, we employed the saline lake-dwelling brine shrimp, *Artemia salina*, as an aquatic animal model [41,48,49]. Wild-type *Vcor* OCN008 was lethal to *Artemia* nauplii (larvae), with a median survival of 53 hours. Inactivation of T6SS2, either alone (Δ*tssM2*) or together with T6SS1 (Δ*hcp1*/Δ*tssM2*), resulted in a significantly reduced lethality (median survival undefined or 56 hours, respectively), whereas inactivation of T6SS1 (Δ*hcp1*) had no effect (**Fig. 4A**). These results reveal a role for the *Vcor* T6SS2 in pathogenicity during infection of a eukaryotic host.

To further investigate the anti-eukaryotic activity of *Vcor* T6SS2 in all three strains, we used real-time microscopy to monitor *Vcor*-mediated cell death kinetics. To this end, we employed bone marrow-derived macrophages (BMDMs), which have been previously used as a model to monitor the toxic effects of another *Vibrio* T6SS [40]. Various levels of cell death were observed starting ~30 minutes after adding either of the wild-type *Vcor* strains BAA-450, OCN008, or OCN014 (**Fig. 4B-D**). Remarkably, inactivation of T6SS2, either alone (Δ*tssM2*) or together with T6SS1 (Δ*hcp1*/Δ*tssM2*), completely abrogated the *Vcor*-mediated cell death, whereas inactivation of T6SS1 (Δ*hcp1*) had no or mild effect. These results support our hypothesis that *Vcor* T6SS2 targets eukaryotes.

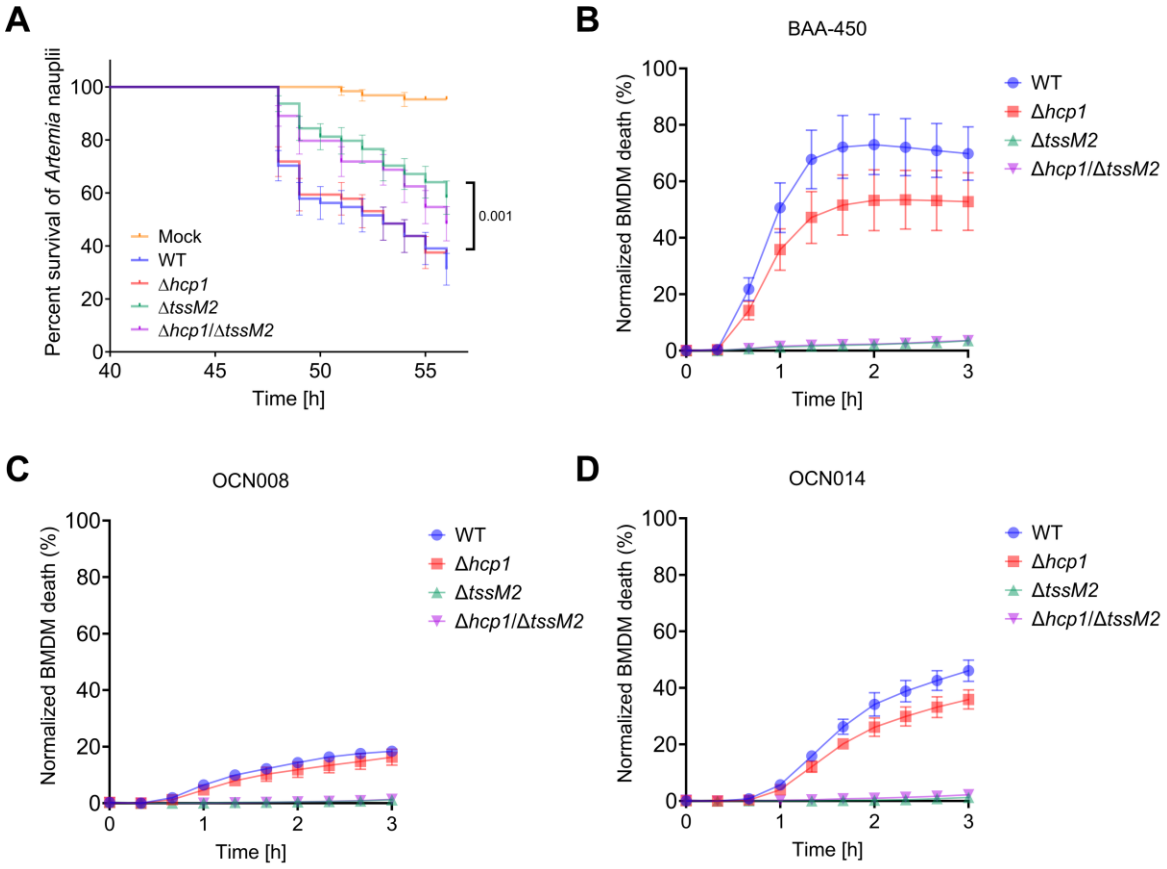

Fig. 4. *Vibrio coralliilyticus* T6SS2 mediates lethality in *Artemia* nauplii and in macrophages. A) *Artemia* nauplii were challenged with the indicated *Vcor* OCN008 strains, and survival was assessed 40 to 56 hours post-infection. Approximately $5x10^7$ bacteria were added to each well containing 2 nauplii. Data are shown as the mean ± SE of four biological replicates, each comprising 16 nauplii for every bacterial strain. The statistical significance between the WT and Δ*tssM2* curves was calculated using the Log-rank (Mantel-Cox) test. **B-D)** Assessment of cell death upon infection of bone marrow-derived macrophages (BMDMs) with the indicated *Vcor* BAA-450 (B), OCN008 (C), or OCN014 (D) strains. Approximately $3.5x10^4$ BMDMs were seeded into 96-well plates in triplicates and infected with *Vcor* strains at a multiplicity of infection (MOI) ~ 4. Propidium iodide (PI) was added to the medium prior to infection, and its uptake kinetics were assessed using real-time microscopy. WT, wild-type. Results from a representative experiment out of at least three independent experiments are shown in B-D.

T6SS1 and T6SS2 secrete diverse effector arsenals

Next, we performed comparative proteomics analyses to reveal the *Vcor* T6SS secretomes and identify the effectors that mediate the antibacterial and anti-eukaryotic activities described above. Using mass spectrometry, we compared the proteins secreted by the wild-type *Vcor* strains BAA-450, OCN008, and OCN014 with those secreted by their isogenic mutants in which either T6SS1 or T6SS2 have been inactivated (Δ*hcp1* or Δ*tssM2*, respectively).

T6SS1 secretomes: We identified eleven, six, and eleven proteins that were significantly enriched in the secretomes of wild-type strains BAA-450, OCN008, and OCN014, respectively, compared to their T6SS1⁻ (Δ*hcp1*) mutants (**Fig. 5**, **Table 1**, and **Dataset S3-S5**). These include the secreted tube-spike structural components Hcp1 (which was deleted to inactivate T6SS1), VgrG1, and PAAR-like proteins. Most of the additional proteins are predicted antibacterial or anti-eukaryotic effectors, or proteins encoded next to them, including: (i) homologs of previously described T6SS effectors, with predicted toxic domains that target the peptidoglycan (e.g., WP_006961156.1 and WP_006961879.1); (ii) proteins containing MIX domains, which are markers for T6SS effectors [45], with predicted nuclease or pore-forming toxic domains (e.g., WP_039951132.1 and WP_201765497.1); and (iii) proteins that have yet to be described as related to T6SSs, which were identified only in the T6SS1 secretome of strain OCN008 (e.g., WP_021456284.1 and WP_021455387.1, which is a DEAD/DEAH box helicase). In accordance with our observation that the T6SS1 appears less active in strain OCN008 compared to the two other *Vcor* strains under the assay conditions (**Fig. 2A**), the comparative proteomics intensity difference for the putative OCN008 T6SS1 effectors was low (**Fig. 5B**), suggesting that the latter type of proteins detected only in the OCN008 T6SS1 secretome may be false positives. As previously reported for similar T6SSs in other vibrios [26,28,45,50], some of the identified proteins are encoded within the T6SS1 gene cluster, whereas others are encoded in auxiliary or orphan operons. Moreover, predicted antibacterial effectors are encoded next to putative immunity genes. Taken together, these results support our findings that *Vcor* T6SS1 plays a role in interbacterial competitions using antibacterial effectors. Interestingly, in each *Vcor* strain, we also identified a secreted MIX domain-containing effector that we previously showed or hypothesized targets eukaryotes rather than bacteria (e.g., WP_006962196.1) [22]. This finding suggests that T6SS1 also plays a role in interactions with eukaryotes, even though our experiments did not reveal significant T6SS1-mediated anti-eukaryotic effects.

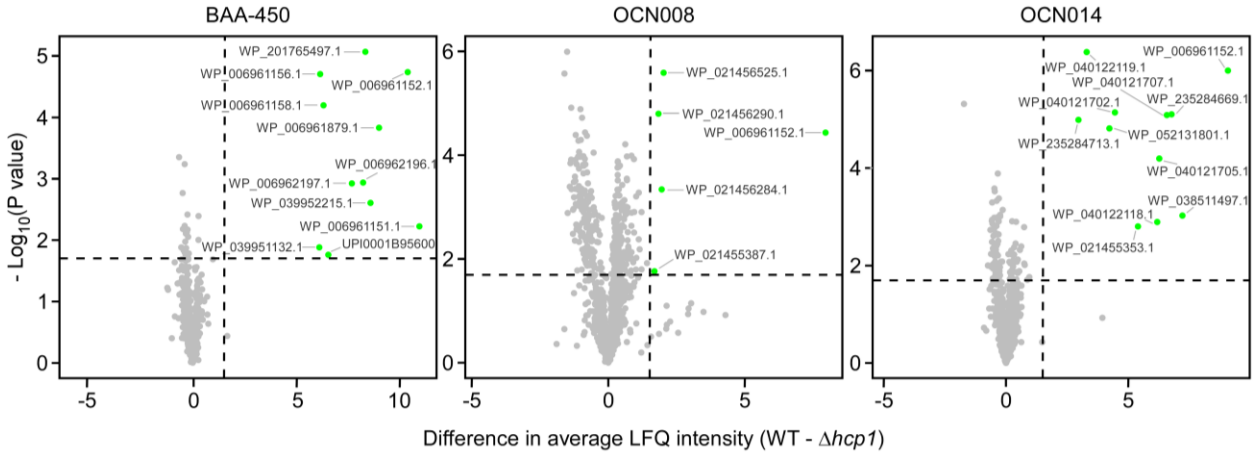

Fig. 5. *Vibrio coralliilyticus* T6SS1 effector repertoires. Volcano plots summarizing the comparative proteomics of proteins identified in the media of the three indicated *Vcor* strains with an active T6SS1 (WT, wild-type) or an inactive T6SS1 (Δ*hcp1*), using label-free quantification (LFQ). The average LFQ signal intensity difference between the WT and Δ*hcp1* strains is plotted against the -Log_{10} of Student's *t* test *P* values (*n* = 3 biological replicates).

Proteins that were significantly more abundant in the secretome of the WT strains (difference in average LFQ intensities > 1.6; *P* value < 0.02; with a minimum of two Razor unique peptides and Score > 15) are denoted in green.

Table 1. *Vibrio coralliilyticus* T6SS1 secretomes identified by comparative proteomics

Predicted role	Predicted activity or domain	BAA-450		OCN008		OCN014	
		Protein accession	Gene locus	Protein accession	Gene locus	Protein accession	Gene locus
T6SS structural	Hcp	WP_006961152.1	VIC_RS16330	WP_006961152.1	G3U99_RS23805	WP_006961152.1	JV59_RS20030
	VgrG	WP_006961151.1	VIC_RS16325	N/D	N/D	WP_040121702.1	JV59_RS20025
	PAAR-like (DUF4150)	WP_039952215.1	VIC_RS19185	N/D	N/D	WP_040122118.1	JV59_RS22990
	PAAR-like (DUF4150)	UPI0001B95600 (annotated as a pseudogene in RefSeq)	VIC_RS08805	WP_021455353.1	G3U99_RS15395	WP_021455353.1	JV59_RS10110
Antibacterial effector	VP1390-like	WP_006961156.1	VIC_RS16350	WP_021456525.1	G3U99_RS23785	WP_040121705.1	JV59_RS20045
	Lysozyme-like	WP_006961879.1	VIC_RS19190	N/A	N/A	WP_040122119.1	JV59_RS22995
	MIX domain; TMs	WP_201765497.1	VIC_RS12080	N/D	N/D	WP_235284713.1	JV59_RS24085
	MIX domain; Pyocin_S; Colicin E9-like nuclease	WP_039951132.1	VIC_RS01010	N/A	N/A	N/A	N/A
	MIX domain; Colicin A-like pore-forming	N/A	N/A	N/A	N/A	WP_052131801.1	JV59_RS24930
	Unknown	N/A	N/A	WP_021456284.1	G3U99_RS12660	N/A	N/A
Anti-eukaryotic effector	MIX domain	WP_006962196.1	VIC_RS20535	N/A	N/A	N/A	N/A
	MIX domain	N/A	N/A	WP_021456290.1	G3U99_RS26335	WP_235284669.1	JV59_RS27320
Effector accessory	MIX domain-containing co-effector	WP_006961158.1	VIC_RS16360	N/D	N/D	WP_040121707.1	JV59_RS20055
	Encoded upstream of anti-eukaryotic MIX domain-containing effector	WP_006962197.1	VIC_RS20540	N/D	N/D	WP_038511497.1	JV59_RS07245
Unknown	DEAD/DEAH box helicase	N/D	N/D	WP_021455387.1	G3U99_RS17670	N/A	N/A

N/A, no homolog is encoded in the genome; N/D, a homolog is encoded in the genome but not detected in the mass-spectrometry analysis; TM, transmembrane helix (according to phobius)

T6SS2 secretomes: We identified ten, nine, and six proteins that were significantly enriched in the secretomes of wild-type strains BAA-450, OCN008, and OCN014, respectively, compared to their T6SS2^{-} (Δ*tssM2*) mutants (**Fig. 6**, **Table 2**, and **Dataset S3-S5**). These include the secreted tube-spike structural components Hcp2 and VgrG2. We predict that all the other identified, non-structural proteins, which are encoded outside the T6SS2 gene cluster (**Fig. S2**), are novel anti-eukaryotic effectors (excluding the phage shock protein, WP_021456780.1, which is probably a phage protein and not a T6SS effector). In support of this prediction, none of these proteins is encoded next to a gene that could encode for a cognate immunity protein. Moreover, some are similar to previously described virulence toxins, such as WP_006960006.1 containing a predicted YopT-like cysteine protease domain (YopT is a type III secretion system virulence effector from *Yersinia* [51]). No putative effectors have a predicted signal peptide for the Sec or Tat secretion systems that could account for their secretion, according to SignalP 6.0 [52] analyses.

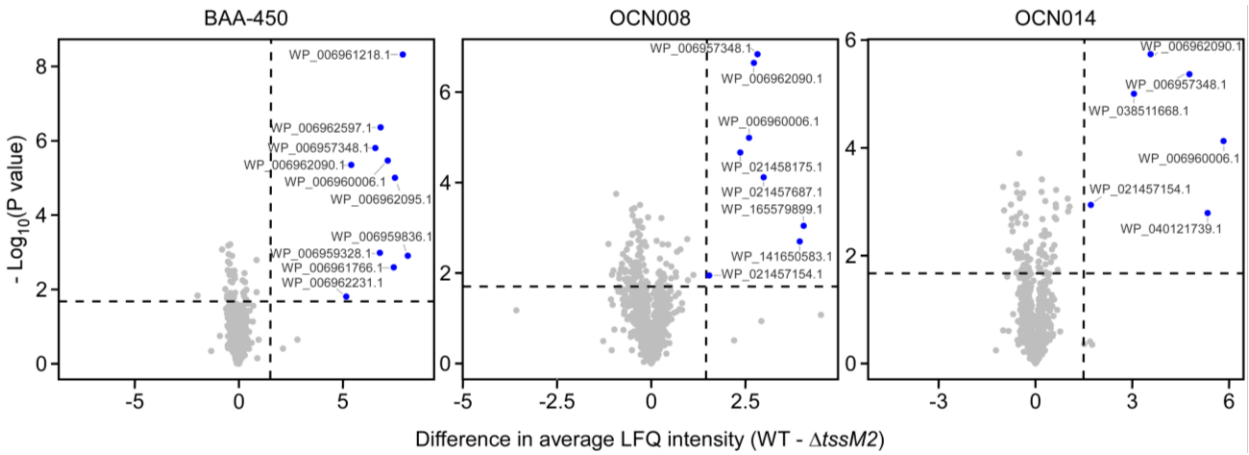

Fig. 6. *Vibrio coralliilyticus* T6SS2 effector repertoires. Volcano plots summarizing the comparative proteomics of proteins identified in the media of the three indicated *Vcor* strains with an active T6SS2 (WT, wild-type) or an inactive T6SS2 (Δ*tssM2*), using label-free quantification (LFQ). The average LFQ signal intensity difference between the WT and Δ*tssM2* strains is plotted against the -Log_{10} of Student's *t* test *P* values (*n* = 3 biological replicates). Proteins that were significantly more abundant in the secretome of the WT strains (difference in average LFQ intensities > 1.6; *P* value < 0.02; with a minimum of two Razor unique peptides and Score > 15) are denoted in blue.

Table 2. *Vibrio coralliilyticus* T6SS2 secretomes identified by comparative proteomics

Predicted role	Predicted activity or domain	BAA-450		OCN008		OCN014	
		Protein accession	Gene locus	Protein accession	Gene locus	Protein accession	Gene locus
T6SS structural	Hcp	WP_006962090.1	VIC_RS20130	WP_006962090.1	G3U99_RS13135	WP_006962090.1	JV59_RS07745
	VgrG	WP_006962095.1	VIC_RS20150	WP_021458175.1	G3U99_RS13110	WP_038511668.1	JV59_RS07720
Anti-eukaryotic effector	CNF-like [a] (CoVe1)	WP_006957348.1	VIC_RS01360	WP_006957348.1	G3U99_RS07885	WP_006957348.1	JV59_RS02730
	(p)ppGpp synthetase / hydrolase [a] (CoVe2)	WP_006959328.1	VIC_RS09310	WP_021457154.1	G3U99_RS15865	WP_021457154.1	JV59_RS10570
	Cysteine peptidase [a] (CoVe3)	WP_006959836.1	VIC_RS11210	N/D	N/D	N/D	N/D
	peptidase_C58-like super family [b]; TM (CoVe4)	WP_006960006.1	VIC_RS11685	WP_006960006.1	G3U99_RS19905	WP_006960006.1	JV59_RS23695
	Unknown (CoVe5)	WP_006961218.1	VIC_RS16620	WP_165579899.1	G3U99_RS23535	WP_040121739.1	JV59_RS20315
	ADP-ribosyltransferase [b] (CoVe6)	WP_006961766.1	VIC_RS18765	WP_021457687.1	G3U99_RS21080	N/A	N/A
	Peptidase_26-like [b] (CoVe7)	WP_006962231.1	VIC_RS20705	N/D	N/D	N/D	N/D
	TM (CoVe8)	WP_006962597.1	VIC_RS22130	N/D	N/D	N/D	N/D
	Unknown (CoVe9)	N/A	N/A	WP_141650583.1	G3U99_RS19765	N/A	N/A
Unknown	Phage shock protein PspA	N/D	N/D	WP_021456780.1	G3U99_RS10060	N/D	N/D

N/A, no homolog is encoded in the genome; N/D, a homolog is encoded in the genome but not detected in the mass-spectrometry analysis; TM, transmembrane helix (according to phobius); [a], according to HHpred; [b], according to NCBI CDD

T6SS2 effectors are novel anti-eukaryotic toxins

Since most of the T6SS1 effectors we identified are homologs of previously described effectors, we focused on the novel T6SS2 effectors for subsequent analyses. Altogether, the identified *Vcor* T6SS2 effector repertoire comprises nine putative novel effectors, which we named *Coralliilyticus* Virulence effector 1 to 9 (CoVe1-9): CoVe1, 2, 4, and 5 were identified in the secretomes of all three strains; CoVe6 was identified in the secretomes of BAA-450 and OCN008; CoVe3, 7, and 8 were identified only in the secretome of BAA-450; and CoVe9 was identified only in the secretome of OCN008 (**Table 2**).

Six of the nine CoVes contain domains with predicted toxic activities (**Table 2**), including peptidase [51], ADP-ribosyltransferase [53], cytotoxic necrotizing factor (CNF)-like deamidase [54], and (p)ppGpp synthetase/hydrolase [55]. However, CoVe5, 8, and 9 sequence analyses did not reveal significant similarity to any previously investigated toxin, suggesting that they harbor novel toxic domains.

We sought to investigate these putative effectors. First, we set out to further validate their T6SS2-dependent secretion using a standard secretion assay. To this end, we cloned the nine putative effectors (CoVe1-8 from strain BAA-450 and CoVe9 from strain OCN008) into an arabinose-inducible expression plasmid, fused to a C-terminal FLAG tag, and monitored their secretion to the media from *Vcor* strains. As shown in **Fig. S3**, T6SS2-dependent secretion of all CoVes, except CoVe3, was evident upon ectopic over-expression from a plasmid in their respective encoding *Vcor* strain. Since CoVe3 T6SS2-dependent secretion was observed in the more sensitive comparative proteomics approach when endogenously expressed from the bacterial chromosome (**Fig. 6**), it is possible that its over-expression from a plasmid hampered the secretion; alternatively, the C-terminal tag that we added to allow CoVe immunoblot detection may have interfered with CoVe3 secretion.

Next, we tested our hypothesis that these novel effectors target eukaryotes. In support of this hypothesis, we found that all nine effectors are toxic when ectopically expressed from a galactose-inducible plasmid in a eukaryotic heterologous model organism, the yeast *Saccharomyces cerevisiae* [56,57] (**Fig. 7A**). In contrast, these effectors were not toxic when expressed from an arabinose-inducible plasmid in *E. coli*, used as a surrogate model bacterium (**Fig. 7B** and **Fig. S4**). These results indicate that T6SS2 secretes an arsenal of novel effectors with anti-eukaryotic activities.

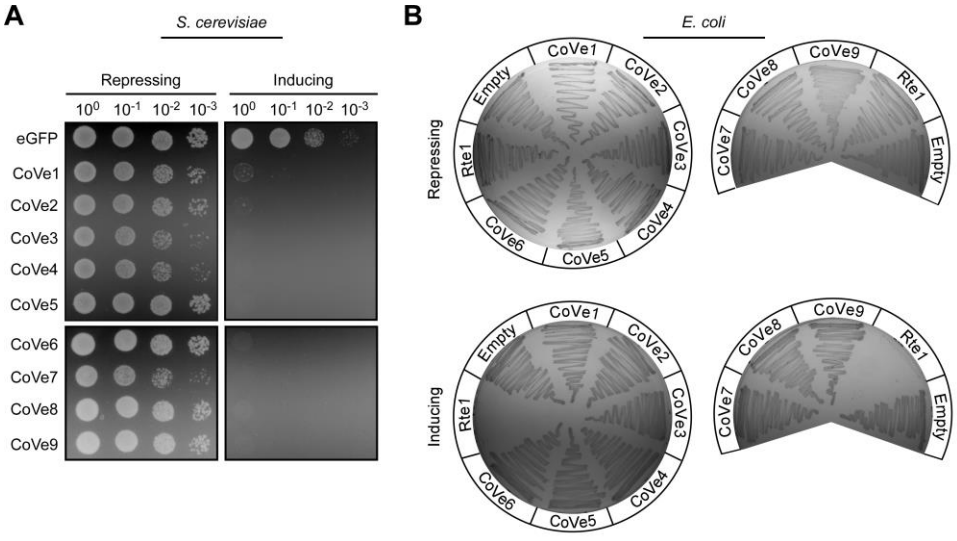

Fig. 7. *Vibrio coralliilyticus* T6SS2 effectors are toxic in eukaryotic cells. A) CoVes are toxic in yeast. Tenfold serial dilutions of *Saccharomyces cerevisiae* strains containing plasmids for the galactose-inducible expression of the indicated CoVes, or eGFP used as a negative control, were spotted on repressing (2% [wt/vol] glucose) or inducing (2% [wt/vol] galactose and 1% [wt/vol] raffinose) agar plates. eGFP, enhanced GFP. **(B)** CoVes are not toxic to bacteria. *Escherichia coli* strains containing plasmids for the arabinose-inducible expression of the indicated, C-terminally FLAG-tagged CoVes, the *V. campbellii* antibacterial T6SS effector Rte1 used as a positive control, or an empty plasmid (Empty) were streaked onto repressing (0.4% [wt/vol] glucose) or inducing (0.001% [wt/vol] arabinose) agar plates. Results from a representative experiment out of at least three independent experiments are shown.

T6SS2 effectors are differentially distributed in Vibrio coralliilyticus genomes

We and others previously showed that T6SS effector repertoires can be divided into core effectors present in all strains harboring the system and accessory effectors encoded only by a subset of strains [25,58,59]. Therefore, we sought to determine the distribution of CoVes in *Vcor* genomes. Interestingly, seven of the nine CoVes are found in all available RefSeq *Vcor* genomes (**Fig. 8** and **Dataset S6**). We propose that these seven CoVes constitute the core effector repertoire of the *Vcor* T6SS2. In contrast, two effectors, CoVe6 and CoVe9, are found only in a subset of strains, suggesting that they are part of the accessory T6SS2 effector repertoire. Interestingly, homologs of CoVe2 and CoVe8 are also found in all *Vcor* genomes (**Fig. S2** and **Dataset S6**). Even though these homologs were not identified in our comparative proteomics analyses, it is possible that they are also T6SS2 effectors.

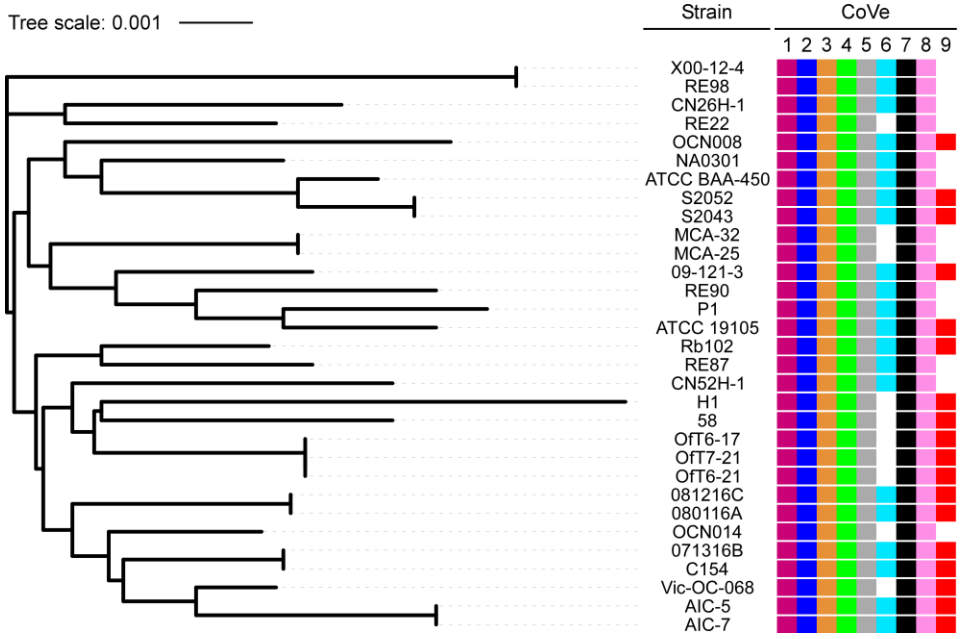

Fig. 8. The *Vibrio coralliilyticus* T6SS2 effector repertoire can be divided into core and accessory arsenals. Distribution of T6SS2 CoVe1-9 effectors in RefSeq *Vcor* genomes. The phylogenetic tree is based on DNA sequences of *rpoB*, coding for DNA-directed RNA polymerase subunit β. The evolutionary history was inferred using the neighbor-joining method.

Discussion

Vibrio coralliilyticus (*Vcor*) is a pathogen that inflicts devastating ecological and economic losses. Although environmental conditions, such as high temperatures, have been associated with increased virulence and a pathogenic lifestyle, the exact virulence factors it uses remain poorly understood. Here, we systematically analyzed the T6SSs in the *Vcor* pan-genome. We revealed two omnipresent T6SSs, T6SS1 and T6SS2, which are regulated by temperature and appear to contribute to *Vcor* virulence. Whereas T6SS1 mediates antibacterial toxicity and thus possibly contributes to host colonization indirectly, T6SS2 secretes an array of novel anti-eukaryotic effectors and appears to play a direct role in virulence.

T6SS1 plays a role in interbacterial competition, possibly contributing to the elimination of host microbiota during host colonization. The T6SS1 effectors identified in our comparative proteomics analyses are homologs of effectors previously reported in similar T6SSs of other vibrios [22,28,45,60] or that have been predicted based on the presence of the MIX domain that defines a widespread class of polymorphic T6SS effectors [22,45]. Therefore, we did not investigate these effectors further in this work.

A recent report implicated prophage induction by LodAB-mediated hydrogen peroxide production as a mechanism *Vcor* uses to outcompete non-pathogenic competitors in the host [61]. Although it is plausible that such competition is mediated by a combination of contact-independent mechanisms, such as the abovementioned prophage induction, and contact-dependent mechanisms, such as the T6SS1-mediated competition, the *Vcor* strains investigated in our study lack LodAB homologs. Moreover, an Orthologous average nucleotide identity (orthoANI) analysis suggested that the SCSIO 43001 strain containing LodAB does not belong to the *Vcor* species (**Dataset S1**). Therefore, we propose that the omnipresent, antibacterial T6SS1 plays a major role in the ability of pathogenic *Vcor* strains to colonize their host.

T6SS2 secretes an array of anti-eukaryotic effectors and mediates toxicity during infection of a model host, *Artemia* nauplii, and during infection of macrophages. Because T6SS2 is induced at high temperatures, in correlation with the onset of *Vcor* virulence, we propose that it plays a role in the colonization and toxicity towards its natural hosts, coral and shellfish larvae. In future work, we will investigate the contribution of T6SS2 to *Vcor*'s virulence in these natural hosts, and we will also determine whether it targets the coral itself or its endosymbiotic dinoflagellates.

Notably, only a few anti-eukaryotic T6SS effectors are known [35,36]. Although we recently revealed anti-eukaryotic effectors in vibrios, belonging to the RIX effector class [42], the CoVes do not belong to any known polymorphic effector class and appear to be new T6SS effectors that have not been previously described. Even though their activities and cellular targets remain to be investigated, six CoVes harbor putative catalytic domains that have previously been implicated in virulence. Future investigations will reveal their mechanism of action and target inside eukaryotic cells.

Although we did not observe T6SS2 secretion in the poor GASW media in *Vcor* OCN008, this system contributed to this strain's virulence during the infection of *Artemina* nauplii. Because the *Artemia* infection assays were also performed in poor media (i.e., Instant Ocean), an unknown host factor possibly contributes to the system's activation during infection. Notably, our results suggest that additional factors contribute to the virulence towards *Artemia*, since inactivation of T6SS2 did not completely abolish toxicity in this host. Interestingly, the results of the BMDM infection assays indicate that the *Vcor* T6SS2 is also active at high temperatures of 37°C, which are infrequent in marine environments. It appears that under these conditions, the anti-eukaryotic toxicity of *Vcor* strains is mediated predominantly by T6SS2, since its inactivation abrogated toxicity to BMDMs. This observation suggests that *Vcor* might also be virulent to

warm-blooded organisms, although, at this time, we have no direct evidence to support this hypothesis.

Materials and Methods

Strains and media: For a complete list of strains used in this study, see **Table S1**. *Escherichia coli* strain DH5α (λ-pir) was grown in 2xYT broth (1.6% [wt/vol] tryptone, 1% [wt/vol] yeast extract, and 0.5% [wt/vol] NaCl) or on Lysogeny broth (LB) agar plates (1.5% [wt/vol]) at 37°C. The media were supplemented with chloramphenicol (10 µg/ml) to maintain plasmids when needed. To repress expression from arabinose-inducible P*bad* promoters, 0.4% (wt/vol) D-glucose was added to the media. To induce expression from P*bad*, L-arabinose was added to the media at 0.001 or 0.1% (wt/vol), as indicated.

Vibrio coralliilyticus (*Vcor*) strains ATCC BAA-450, OCN008 and OCN014, and their derivatives were grown in Marine Lysogeny broth (MLB; LB containing 3% [wt/vol] NaCl) or on GASW-Tris agar plates (20.8 [g/l] NaCl, 0.56 [g/l] KCl, 4.8 [g/l] $MgSO_4 \cdot 7H_2O$, 4 [g/l] $MgCl_2 \cdot 6H_2O$, 0.01 [g/l] K_2HPO_4, 0.001 [g/l] $FeSO_4 \cdot 7H_2O$, 2 [g/l] Instant Ocean sea salts, 6.33 [g/l] Tris base [$C_4H_{11}NO_3$], 4 [g/l] tryptone, 2 [g/l] yeast extract, 0.2% [vol/vol] glycerol, and 1.5% [wt/vol] agar; pH was adjusted to 8.3 with HCl) at 30°C. For colony selection after plasmid conjugation (see below), *Vcor* was grown on TCBS agar (Millipore, #86348) plates. L-arabinose (0.01% [wt/vol]) was added to the media to induce expression from P*bad*.

Vibrio natriegens ATCC 14048 were grown on Marine Minimal Media (MMM) agar plates (2% [wt/vol] NaCl, 0.4% [wt/vol] galactose, 5 mM $MgSO_4$, 7 mM K_2SO_4, 77 mM K_2HPO_4, 35 mM KH_2PO_4, 2 mM NH_4Cl, and 1.5% [wt/vol] agar) at 30°C. The media were supplemented with chloramphenicol (10 µg/ml) to select for or maintain plasmids when necessary.

Saccharomyces cerevisiae were grown in Yeast Extract–Peptone–Dextrose broth (YPD; 1% [wt/vol] yeast extract, 2% [wt/vol] peptone, and 2% [wt/vol] glucose) or on YPD agar plates (2% [wt/vol]) at 30°C. Yeast containing plasmids that provide prototrophy to leucine were grown in Synthetic Dropout media (SD; 6.7 [g/l] yeast nitrogen base without amino acids, 1.4 [g/l] yeast synthetic dropout medium supplement (Sigma)) supplemented with histidine (2 [ml/l] from a 1% [wt/vol] stock solution), tryptophan (2 [ml/l] from a 1% [wt/vol] stock solution), uracil (10 [ml/l] from a 0.2% [wt/vol] stock solution), and glucose (4% [wt/vol]). For galactose-inducible expression from a plasmid, cells were grown in SD media or on SD agar plates supplemented with galactose (2% [wt/vol]) and raffinose (1% [wt/vol]).

Plasmid construction: For a complete list of plasmids used in this study, see **Table S2**. For a complete list of primers used in this study, see **Table S3**. To enable strong, arabinose-inducible protein expression in *Vcor*, we constructed the plasmid pKara1. To this end, we amplified the region between the *araC* cassette and *rrnB* T1 terminator, including a C-terminally FLAG-tagged sfGFP gene, from the plasmid psfGFP [60], and introduced it 220 bp upstream of the gene encoding the fluorescent protein DsRed in pVSV208 [62], using the Gibson assembly method.

For expression in bacteria, the coding sequences (CDS) of the indicated genes of interest were amplified by PCR from the respective genomic DNA of the encoding bacterium. Next, amplicons were inserted into the multiple cloning site (MCS) of pBAD33.1^F, or in place of the sfGFP gene within pKara1, using the Gibson assembly method [63], in-frame with the C-terminal FLAG tag. Plasmids were introduced into *E. coli* DH5α (λ-pir) by electroporation and into vibrios via conjugation. Transconjugants were selected on TCBS agar (Millipore) plates supplemented with chloramphenicol and then counter-selected on GASW agar plates containing chloramphenicol.

For galactose-inducible expression in yeast, genes were inserted into the MCS of the shuttle vector pGML10 (Riken) using the Gibson assembly method, in-frame with a C-terminal Myc tag. Yeast transformations were performed using the lithium acetate method, as described previously [64].

Construction of deletion strains: To delete genes in *Vcor* BAA-450, OCN008, and OCN014, 1 kb sequences upstream and downstream of each gene to be deleted were cloned together into the MCS of pDM4, a Cm^ROriR6K suicide plasmid. The pDM4 constructs were transformed into *E. coli* DH5α (λ-pir) by electroporation and then conjugated into *Vcor* strains. Transconjugants were selected on TCBS agar plates supplemented with chloramphenicol and then counter-selected on agar plates containing 15% (wt/vol) sucrose for loss of the *sacB*-containing plasmid. Deletions were confirmed by PCR.

***Vibrio* protein secretion assays:** Secretion and expression assays were performed as previously reported [24], with minor modifications. *Vcor* strains were grown for 16 hours in MLB supplemented with antibiotics to maintain plasmids when necessary. Bacterial cultures were diluted four-fold in fresh media and incubated for two additional hours at 28°C. Then, the cultures were normalized to an optical density at 600 nm (OD_{600}) of 0.18 in 5 ml of MLB or GASW media, as indicated. When protein expression from an arabinose-inducible plasmid was required, the media were supplemented with chloramphenicol and 0.01% (wt/vol) L-arabinose. The cultures were then incubated with continuous shaking (220 rpm) at 19°C, 23°C, 28°C or 31°C, as indicated, for four hours. For expression fractions, 0.5 OD_{600} units were harvested, and cell pellets were resuspended in 30 µl of 2x Tris-glycine SDS sample buffer (Novex, Life Sciences) with 5% (vol/vol) β-mercaptoethanol. For secretion fractions, supernatant volumes equivalent to 5 OD_{600} units were filtered (0.22 µm), and proteins were precipitated using the deoxycholate and trichloroacetic acid method [65]. The precipitated proteins were washed twice with cold acetone and air-dried before being resuspended in 20 µl of 100 mM Tris-Cl (pH = 8.0) and 20 µl of 2x Tris-glycine SDS sample buffer containing 5% (vol/vol) β-mercaptoethanol. Protein samples were incubated at 95°C for 10 minutes before being resolved on TGX Stain-free gels (Bio-Rad). The proteins were transferred onto 0.2 µm nitrocellulose membranes using Trans-Blot Turbo Transfer (Bio-Rad), following the manufacturer's protocol. Membranes were then immunoblotted with custom-made α-Hcp2 (GenScript; polyclonal antibodies raised in rabbits against the peptides CGEGGKIEKGPEVGF or CVMTKPNREGSGADP; the latter was used only in the experiment shown in Fig. 2A), Custom-made polyclonal α-VgrG1 [66], monoclonal α-FLAG (Sigma-Aldrich, F1804), or Direct-Blot™ HRP anti-*E. coli* RNA polymerase sigma 70 (mouse mAb #663205; BioLegend; referred to as α-RNAP) antibodies at a dilution of 1:1000. Protein signals were detected using enhanced chemiluminescence (ECL) reagents with a Fusion FX6 imaging system (Vilber Lourmat).

Mass spectrometry analyses: Sample preparations for mass spectrometry were performed as described in the "*Vibrio* protein secretion assays" section. After the acetone wash step, samples were shipped to the Smoler Proteomics Center at the Technion, Israel, for analysis. Precipitated proteins were washed twice in 80% (vol/vol) cold acetone. The protein pellets were dissolved in 8.5 M Urea, 400 mM ammonium bicarbonate, and 10 mM DTT. Protein concentrations were estimated using the Bradford assay. The proteins were reduced at 60ºC for 30 minutes and then modified with 35.2 mM iodoacetamide in 100 mM ammonium bicarbonate for 30 minutes at room temperature in the dark. The proteins were digested overnight at 37ºC in 1.5 M urea and 66 mM ammonium bicarbonate with modified trypsin (Promega) at a 1:50 (M/M) enzyme-to-substrate ratio. An additional trypsinization step was performed for four hours. The resulting tryptic peptides were analyzed by LC-MS/MS using Q Exactive HF mass spectrometer (Thermo) fitted with a capillary HPLC (Evosep). The peptides were loaded onto a 15 cm ID 150 1.9-micron (Batch no. E1121-3-24) column of Evosep. The peptides were eluted with the built-in

Xcalibur 15 SPD (88 min) method. Mass spectrometry was performed in a positive mode using repetitively full MS scan (m/z 350–1200) followed by High energy Collision Dissociation (HCD) of the 20 most dominant ions selected from the full MS scan. A dynamic exclusion list was enabled with exclusion duration of 20 seconds.

The mass spectrometry data were analyzed with the MaxQuant software 2.1.1.0 (www.maxquant.org) using the Andromeda search engine [67] against the relevant *Vcor* strains from the Uniprot database, with a mass tolerance of 4.5 ppm for the precursor masses and 4.5 ppm for the fragment ions. Peptide- and protein-level false discovery rates (FDRs) were filtered to 1% using the target-decoy strategy. The protein table was filtered to eliminate identities from the reverse database and common contaminants. The data were quantified by label-free analysis using the same software, based on extracted ion currents (XICs) of peptides, enabling quantitation from each LC/MS run for each peptide identified in any of the experiments. Statistical analyses of the identification and quantization results were done using the Perseus 1.6.7.0 software [68]. The mass spectrometry proteomics data have been deposited in the ProteomeXchange Consortium via PRIDE [69].

Bacterial competition assays: Bacterial competition assays were performed as previously described [24], with minor modifications. Attacker and prey strains were grown for 16 hours in appropriate media. In the morning, *Vcor* attacker strains were diluted 1:10 into fresh media and incubated for an additional hour at 28°C. Attacker and prey cultures were then normalized to an OD_{600} of 0.5 and mixed at a 4:1 (attacker:prey) ratio in triplicate. Next, the mixtures were spotted (25 µl) on MLB agar competition plates and incubated at 28°C for 4 h. The colony-forming units (CFU) of the prey strains at t = 0 h were determined by plating tenfold serial dilutions on selective media plates. After 4 hours of co-incubation on competition plates, the bacteria were harvested, and the CFUs of the surviving prey strains were determined as described above. Prey strains contained a pBAD33.1 plasmid to allow selective growth on plates containing chloramphenicol.

***Vibrio coralliilyticus* growth assays:** Triplicates *Vcor* cultures grown for 16 hours were normalized to OD_{600} = 0.01 in MLB and transferred to a 96-well plate (200 µl per well). The 96-well plate was incubated in a microplate reader (BioTek SYNERGY H1) at 28°C with continuous shaking (205 cpm). Growth was measured as OD_{600} in 10-minute intervals.

***Artemia* infection assays:** *Artemia* infection assays were performed as previously reported [41], with minor modifications. *Artemia salina* eggs (Artemio Pur; JBL) were incubated in deionized distilled water containing chloramphenicol (10 µg/ml), kanamycin (100 µg/ml), and ampicillin (100 µg/ml) at 28°C with continuous rotation for an hour. The eggs were washed four times with Instant Ocean solution (3.3% [wt/vol]; Aquarium Systems) and then incubated for 24 hours with continuous rotation at 28°C. Hatched *Artemia* nauplii were transferred into sterile 48-well plates (two nauplii per well in 400 µl Instant Ocean). Approximately $5x10^7$ bacteria were added to each well, and the plates were incubated at 28°C under 12-hour light and dark cycles. *Artemia* survival was determined at the indicated timepoints post-infection. An *Artemia* nauplius that did not move for 10 seconds was defined as non-viable. Each bacterial strain was added to 8 wells (16 nauplii). Survival results are provided as grouped data from four independent experiments. Percent survival was calculated as surviving subjects out of the subjects at risk for each time point.

BMDM infection assays: Bone marrow cells from 6-8 week-old mice were isolated, and bone marrow-derived macrophages (BMDMs) were obtained after a 7-day differentiation, as previously described [70]. *Vcor* strains were grown for 16 hours in MLB. In the morning, bacterial cultures were diluted tenfold into fresh media and incubated for an additional hour at 28°C. Approximately $3.5x10^4$ BMDMs were seeded into 96-well plates in triplicates in 1%

(vol/vol) FBS and penicillin-streptomycin-free DMEM media and then infected with the indicated *Vcor* strains at a multiplicity of infection (MOI) ~ 4. Plates were centrifuged for 5 minutes at 400 x *g*. Propidium iodide (PI; 1 μg/ml) was added to the medium 30 minutes prior to infection, and its uptake kinetics were assessed every 15 minutes using real-time microscopy (Incucyte SX5) during incubation at 37°C. The data were analyzed using the Incucyte SX5 analysis software and exported to Graphpad PRISM. Normalization was performed according to the maximal PI-positive object count to calculate the percentage of dead cells [70].

Yeast toxicity assays: Toxicity assays in yeast were performed as previously described [64]. Briefly, yeast cells were cultured for 16 hours in SD media supplemented with 4% glucose (wt/vol). Bacterial cultures were washed twice with sterile deionized distilled water and normalized to an OD_{600} of 1.0 in sterile deionized water. Then, tenfold serial dilutions were spotted onto SD agar plates containing 4% (wt/vol) glucose (repressing plates) or 2% (wt/vol) galactose and 1% (wt/vol) raffinose (inducing plates). The plates were incubated at 28°C for two days.

Protein expression in *E. coli*: Overnight-grown bacterial cultures of *E. coli* DH5α (λ-pir) strains carrying pBAD33.1 arabinose-inducible expression plasmids were grown in 2xYT broth supplemented with chloramphenicol. Bacterial cultures were normalized to an OD_{600} = 0.5 in 3 ml fresh 2xYT with chloramphenicol and incubated with continuous shaking (220 rpm) at 37°C for 2 hours. Then, L-arabinose was added to a final concentration of 0.1% (wt/vol) to induce protein expression, and the cultures were incubated for two additional hours. Cells equivalent to 0.5 OD_{600} units were harvested, and their pellets were resuspended in 50 μl of 2x Tris-glycine SDS sample buffer (Novex, Life Sciences) supplemented with 5% (vol/vol) β-mercaptoethanol. Subsequently, the samples were boiled at 95°C for 10 minutes and resolved on a TGX stain-free gel (Bio-Rad) for SDS-PAGE analysis. The proteins were transferred onto nitrocellulose membranes, which were then immunoblotted with α-FLAG (Sigma-Aldrich, F1804) antibodies at a 1:1000 dilution. Finally, protein signals were detected using ECL in a Fusion FX6 imaging system (Vilber Lourmat). The loading control for total protein lysates was visualized as the fluorescence of activated trihalo compounds found in the gel.

***E. coli* toxicity assays:** To determine the toxicity of *Vcor* proteins in bacteria, *E. coli* DH5α (λ-pir) strains carrying pBAD33.1 arabinose-inducible expression plasmids were streaked onto LB agar plates supplemented with chloramphenicol and either 0.4% (wt/vol) glucose (repressing plates) or 0.001% (wt/vol) L-arabinose (inducing plates). Plates were incubated for 16 hours at 37°C.

Identifying T6SS gene clusters in *Vibrio coralliilyticus*: A local database containing the RefSeq bacterial nucleotide and protein sequences was generated (last updated on August 21, 2023). *Vcor* genomes were retrieved from the local database, and OrthoANI [71] was performed as described previously [72]. The *Vcor* strain SCSIO 43001 genome (assembly accession GCF_024449095.1) was removed from the dataset because it showed OrthoANI values <95%. The *Vcor* strain RE22 (assembly accession GCF_001297935.1) was removed because an updated version of strain RE22 was found (assembly accession GCF_003391375.1).

The presence of T6SS gene clusters in *Vcor* genomes was determined by following a two-step procedure described previously [50]. Briefly, in the first step, BLASTN was employed to align *Vcor* nucleotide sequences against the nucleotide sequences of representative T6SS clusters (**Fig. 1** and **Dataset S2**). The best alignments for each nucleotide accession number were saved. In the second step, a two-dimensional matrix was generated for each T6SS gene cluster. The matrices were filled in with the percent identity values based on the positions of the alignments from the first step. The overall coverage was calculated for each T6SS gene cluster

in each genome. *Vcor* genomes with at least 70% overall coverage of a T6SS gene cluster were regarded as containing that T6SS gene cluster (**Dataset S2**).

Identifying effector homologs in *Vibrio coralliilyticus* genomes: BLASTP was employed to identify homologs of the T6SS2 effectors in *Vcor* genomes, as described previously [25]. The amino acid sequences of new CoVes from strains BAA-450 (WP_006957348.1, WP_006959328.1, WP_006959836.1, WP_006960006.1, WP_006961218.1, WP_006961766.1, WP_006962231.1, and WP_006962597.1) and OCN008 (WP_141650583.1) were used as queries. The E-value threshold was set to $10^{-12,}$ and the coverage was set to 70% based on the length of the query sequences.

Constructing a phylogenetic tree: The nucleotide sequences of the *rpoB* gene, coding for DNA-directed RNA polymerase subunit beta, were retrieved from the local RefSeq database. Phylogenetic analyses of bacterial genomes were conducted using the MAFFT 7 server (mafft.cbrc.jp/alignment/server/) as described before [73]. A multiple sequence alignment was generated using MAFFT v7 FFT-NS-I [74,75]. The evolutionary history of *Vcor* genomes was inferred using the neighbor-joining method [76] with the Jukes-Cantor substitution model (JC69). The analysis included 31 nucleotide sequences and 4,029 conserved sites.

Data Availability

The mass spectrometry proteomics data have been deposited in the ProteomeXchange Consortium via the PRIDE [69] partner repository with the dataset identifier PXD049479.

Conflict of Interest

The authors declare no competing interests.

Acknowledgments

This project received funding from the National Science Foundation and United States-Israel Binational Science Foundation (NSF grant number 2207168 and BSF grant number 2021733 to DS, JvK, and BU) and the Israel Science Foundation (ISF grant number 1362/21 to DS and EB, and grant number 2174/22 to MG). We thank members of the Salomon, van Kessel, and Ushijima groups for valuable discussions, and Katarzyna Kanarek for preparing the pKara1 plasmid. We also thank the Smoler Proteomics Center at the Technion for performing and analyzing the mass spectrometry data.

Author contributions

Conceptualization: BU, JvK, and DS; Formal Analysis: SM, HC, EB, and DS; Funding Acquisition: MG, BU, JvK, EB, and DS; Investigation: SM, HC, and EB; Methodology: SM, HC, and EB; Resources: MG, BU, JvK; Supervision: DS; Writing – Original Draft Preparation: SM and DS; Writing – Review and Editing: HC, MG, BU, JvK, and EB.

References

1. Horseman MA, Bray R, Lujan-Francis B, Matthew E. Infections Caused by Vibrionaceae. Infect Dis Clin Pract. 2013;21: 222–232. doi:10.1097/IPC.0b013e3182826328

2. Baker-Austin C, Oliver JD, Alam M, Ali A, Waldor MK, Qadri F, et al. Vibrio spp. infections. Nat Rev Dis Prim. 2018;4: 1–19. doi:10.1038/s41572-018-0005-8

3. Martinez-Urtaza J, Baker-Austin C, Jones JL, Newton AE, Gonzalez-Aviles GD, DePaola A. Spread of Pacific Northwest *Vibrio parahaemolyticus* Strain. N Engl J Med. 2013;369: 1573–1574. doi:10.1056/NEJMc1305535

4. Le Roux F, Wegner KM, Baker-Austin C, Vezzulli L, Osorio CR, Amaro C, et al. The emergence of Vibrio pathogens in Europe: Ecology, evolution and pathogenesis (Paris, 11-12 March 2015). Front Microbiol. 2015;6: 1–8. doi:10.3389/fmicb.2015.00830

5. Vezzulli L, Grande C, Reid PC, Hélaouët P, Edwards M, Höfle MG, et al. Climate influence on *Vibrio* and associated human diseases during the past half-century in the coastal North Atlantic. Proc Natl Acad Sci. 2016;113: E5062–E5071. doi:10.1073/pnas.1609157113

6. Newton A, Kendall M, Vugia DJ, Henao OL, Mahon BE. Increasing Rates of Vibriosis in the United States, 1996–2010: Review of Surveillance Data From 2 Systems. Clin Infect Dis. 2012;54: S391–S395. doi:10.1093/cid/cis243

7. Burke S, Pottier P, Lagisz M, Macartney EL, Ainsworth T, Drobniak SM, et al. The impact of rising temperatures on the prevalence of coral diseases and its predictability: A global meta-analysis. Ecol Lett. 2023;26. doi:10.1111/ele.14266

8. Arboleda M, Reichardt W. Epizoic communities of prokaryotes on healthy and diseased scleractinian corals in Lingayen Gulf, Philippines. Microb Ecol. 2009;57. doi:10.1007/s00248-008-9400-0

9. Moriarty T, Leggat W, Huggett MJ, Ainsworth TD. Coral Disease Causes, Consequences, and Risk within Coral Restoration. Trends in Microbiology. 2020. doi:10.1016/j.tim.2020.06.002

10. Elliff CI, Silva IR. Coral reefs as the first line of defense: Shoreline protection in face of climate change. Marine Environmental Research. 2017. doi:10.1016/j.marenvres.2017.03.007

11. Mera H, Bourne DG. Disentangling causation: complex roles of coral-associated microorganisms in disease. Environmental Microbiology. 2018. doi:10.1111/1462-2920.13958

12. Bender-Champ D, Diaz-Pulido G, Dove S. Effects of elevated nutrients and CO2 emission scenarios on three coral reef macroalgae. Harmful Algae. 2017;65. doi:10.1016/j.hal.2017.04.004

13. Vanwonterghem I, Webster NS. Coral Reef Microorganisms in a Changing Climate. iScience. 2020. doi:10.1016/j.isci.2020.100972

14. Tout J, Siboni N, Messer LF, Garren M, Stocker R, Webster NS, et al. Increased seawater temperature increases the abundance and alters the structure of natural Vibrio populations associated with the coral Pocillopora damicornis. Front Microbiol. 2015;6. doi:10.3389/fmicb.2015.00432

15. Ben-Haim Y, Zicherman-Keren M, Rosenberg E. Temperature-regulated bleaching and lysis of the coral Pocillopora damicornis by the novel pathogen Vibrio coralliilyticus. Appl Environ Microbiol. 2003;69: 4236–42. Available: http://www.ncbi.nlm.nih.gov/pubmed/12839805

16. Ushijima B, Videau P, Burger AH, Shore-Maggio A, Runyon CM, Sudek M, et al. Vibrio

coralliilyticus strain OCN008 is an etiological agent of acute montipora white syndrome. Appl Environ Microbiol. 2014;80. doi:10.1128/AEM.03463-13

17. Richards GP, Watson MA, Needleman DS, Church KM, Häse CC. Mortalities of Eastern And Pacific oyster larvae caused by the pathogens Vibrio coralliilyticus and Vibrio tubiashii. Appl Environ Microbiol. 2015;81. doi:10.1128/AEM.02930-14

18. Ushijima B, Richards GP, Watson MA, Schubiger CB, Häse CC. Factors affecting infection of corals and larval oysters by Vibrio coralliilyticus. PLoS One. 2018;13. doi:10.1371/journal.pone.0199475

19. Kimes NE, Grim CJ, Johnson WR, Hasan NA, Tall BD, Kothary MH, et al. Temperature regulation of virulence factors in the pathogen Vibrio coralliilyticus. ISME J. 2012;6: 835–846. doi:10.1038/ismej.2011.154

20. Childers BM, Klose KE. Regulation of virulence in Vibrio cholerae: The ToxR regulon. Future Microbiology. 2007. doi:10.2217/17460913.2.3.335

21. Ushijima B, Videau P, Poscablo D, Stengel JW, Beurmann S, Burger AH, et al. Mutation of the toxR or mshA genes from Vibrio coralliilyticus strain OCN014 reduces infection of the coral Acropora cytherea. Environ Microbiol. 2016;18. doi:10.1111/1462-2920.13428

22. Dar Y, Salomon D, Bosis E. The antibacterial and anti-eukaryotic Type VI secretion system MIX-effector repertoire in Vibrionaceae. Mar Drugs. 2018;16: 433. doi:10.1016/bs.ctdb.2015.10.001

23. Pukatzki S, Ma AT, Sturtevant D, Krastins B, Sarracino D, Nelson WC, et al. Identification of a conserved bacterial protein secretion system in Vibrio cholerae using the Dictyostelium host model system. Proc Natl Acad Sci. 2006;103: 1528–1533. doi:10.1073/pnas.0510322103

24. Salomon D, Gonzalez H, Updegraff BL, Orth K. Vibrio parahaemolyticus Type VI secretion system 1 Is activated in marine conditions to target bacteria, and is differentially regulated from system 2. PLoS One. 2013;8: e61086. doi:10.1371/journal.pone.0061086

25. Tchelet D, Keppel K, Bosis E, Salomon D. Vibrio parahaemolyticus T6SS2 effector repertoires. Gut Microbes. 2023;15. doi:10.1080/19490976.2023.2178795

26. Salomon D, Klimko JA, Trudgian DC, Kinch LN, Grishin N V., Mirzaei H, et al. Type VI secretion system toxins horizontally shared between marine bacteria. PLoS Pathog. 2015;11: 1–20. doi:10.1371/journal.ppat.1005128

27. Speare L, Cecere AG, Guckes KR, Smith S, Wollenberg MS, Mandel MJ, et al. Bacterial symbionts use a type VI secretion system to eliminate competitors in their natural host. Proc Natl Acad Sci U S A. 2018;115: E8528–E8537. doi:10.1073/pnas.1808302115

28. Ray A, Schwartz N, Souza Santos M, Zhang J, Orth K, Salomon D, et al. Type VI secretion system MIX-effectors carry both antibacterial and anti-eukaryotic activities. EMBO Rep. 2017;18: e201744226. doi:10.15252/embr.201744226

29. Piel D, Bruto M, James A, Labreuche Y, Lambert C, Janicot A, et al. Selection of Vibrio crassostreae relies on a plasmid expressing a type 6 secretion system cytotoxic for host immune cells. Environ Microbiol. 2020;22. doi:10.1111/1462-2920.14776

30. Wang J, Brodmann M, Basler M. Assembly and subcellular localization of bacterial type VI secretion systems. Annu Rev Microbiol. 2019;73. doi:10.1146/annurev-micro-020518-115420

31. Jana B, Salomon D. Type VI secretion system: a modular toolkit for bacterial dominance.

Future Microbiol. 2019;14: fmb-2019-0194. doi:10.2217/fmb-2019-0194

32. Hernandez RE, Gallegos-Monterrosa R, Coulthurst SJ. Type VI secretion system effector proteins: Effective weapons for bacterial competitiveness. Cellular Microbiology. 2020. doi:10.1111/cmi.13241

33. Allsopp LP, Bernal P. Killing in the name of: T6SS structure and effector diversity. Microbiology. 2023;169: 001367. doi:10.1099/MIC.0.001367

34. Basler M, Pilhofer M, Henderson GP, Jensen GJ, Mekalanos JJ. Type VI secretion requires a dynamic contractile phage tail-like structure. Nature. 2012;483: 182–6. doi:10.1038/nature10846

35. Hachani A, Wood TE, Filloux A. Type VI secretion and anti-host effectors. Curr Opin Microbiol. 2016;29: 81–93. doi:10.1016/j.mib.2015.11.006

36. Monjarás Feria J, Valvano MA. An Overview of Anti-Eukaryotic T6SS Effectors. Frontiers in Cellular and Infection Microbiology. 2020. doi:10.3389/fcimb.2020.584751

37. Huang Y, Du P, Zhao M, Liu W, Du Y, Diao B, et al. Functional characterization and conditional regulation of the type VI secretion system in Vibrio fluvialis. Front Microbiol. 2017;8: 1–15. doi:10.3389/fmicb.2017.00528

38. MacIntyre DL, Miyata ST, Kitaoka M, Pukatzki S. The Vibrio cholerae type VI secretion system displays antimicrobial properties. Proc Natl Acad Sci. 2010;107: 19520–19524. doi:10.1073/pnas.1012931107

39. Church SR, Lux T, Baker-Austin C, Buddington SP, Michell SL. Vibrio vulnificus type 6 secretion system 1 contains anti-bacterial properties. PLoS One. 2016;11: 1–17. doi:10.1371/journal.pone.0165500

40. Cohen H, Baram N, Fridman CM, Edry-Botzer L, Salomon D, Gerlic M. Post-phagocytosis activation of NLRP3 inflammasome by two novel T6SS effectors. Elife. 2022;11: e82766.

41. Cohen H, Fridman CM, Gerlic M, Salomon D. A Vibrio T6SS-Mediated Lethality in an Aquatic Animal Model. Cascales E, editor. Microbiol Spectr. 2023;11. doi:10.1128/spectrum.01093-23

42. Kanarek K, Fridman CM, Bosis E, Salomon D. The RIX domain defines a class of polymorphic T6SS effectors and secreted adaptors. Nat Commun 2023 141. 2023;14: 1–13. doi:10.1038/s41467-023-40659-2

43. Bruto M, James A, Petton B, Labreuche Y, Chenivesse S, Alunno-Bruscia M, et al. Vibrio crassostreae, a benign oyster colonizer turned into a pathogen after plasmid acquisition. ISME J. 2017;11: 1043–1052. doi:10.1038/ismej.2016.162

44. Guillemette R, Ushijima B, Jalan M, Häse CC, Azam F. Insight into the resilience and susceptibility of marine bacteria to T6SS attack by Vibrio cholerae and Vibrio coralliilyticus. PLoS One. 2020;15. doi:10.1371/journal.pone.0227864

45. Salomon D, Kinch LN, Trudgian DC, Guo X, Klimko JA, Grishin N V., et al. Marker for type VI secretion system effectors. Proc Natl Acad Sci. 2014;111: 9271–9276. doi:10.1073/pnas.1406110111

46. Ben-Haim Y, Thompson FL, Thompson CC, Cnockaert MC, Hoste B, Swings J, et al. Vibrio coralliilyticus sp. nov., a temperature-dependent pathogen of the coral Pocillopora damicornis. Int J Syst Evol Microbiol. 2003;53. doi:10.1099/ijs.0.02402-0

47. Ushijima B, Videau P, Poscablo D, Vine V, Salcedo M, Aeby G, et al. Complete genome sequence of Vibrio coralliilyticus strain OCN014, isolated from a diseased coral at Palmyra Atoll. Genome Announc. 2014;2. doi:10.1128/genomeA.01318-14

48. Neu AK, Månsson M, Gram L, Prol-García MJ. Toxicity of bioactive and probiotic marine bacteria and their secondary metabolites in artemia sp. and caenorhabditis elegans as eukaryotic model organisms. Appl Environ Microbiol. 2014;80. doi:10.1128/AEM.02717-13

49. Austin B, Austin D, Sutherland R, Thompson F, Swings J. Pathogenicity of vibrios to rainbow trout (Oncorhynchus mykiss, Walbaum) and Artemia nauplii. Environ Microbiol. 2005;7: 1488–1495. doi:10.1111/j.1462-2920.2005.00847.x

50. Jana B, Keppel K, Fridman CM, Bosis E, Salomon D. Multiple T6SSs, mobile auxiliary modules, and effectors revealed in a systematic analysis of the Vibrio parahaemolyticus pan-genome. Bordenstein S, editor. mSystems. 2022; e00723-22. doi:10.1128/MSYSTEMS.00723-22

51. Iriarte M, Cornelis GR. YopT, a new Yersinia Yop effector protein, affects the cytoskeleton of host cells. Mol Microbiol. 1998;29. doi:10.1046/j.1365-2958.1998.00992.x

52. Teufel F, Almagro Armenteros JJ, Johansen AR, Gíslason MH, Pihl SI, Tsirigos KD, et al. SignalP 6.0 predicts all five types of signal peptides using protein language models. Nat Biotechnol. 2022;40. doi:10.1038/s41587-021-01156-3

53. Deng Q, Barbieri JT. Molecular mechanisms of the cytotoxicity of ADP-ribosylating toxins. Annual Review of Microbiology. 2008. doi:10.1146/annurev.micro.62.081307.162848

54. Knust Z, Schmidt G. Cytotoxic necrotizing factors (CNFs)-a growing toxin family. Toxins. 2010. doi:10.3390/toxins2010116

55. Ahmad S, Wang B, Walker MD, Tran HKR, Stogios PJ, Savchenko A, et al. An interbacterial toxin inhibits target cell growth by synthesizing (p)ppApp. Nature. 2019;575: 674–678. doi:10.1038/s41586-019-1735-9

56. Siggers KA, Lesser CF. The Yeast Saccharomyces cerevisiae: A Versatile Model System for the Identification and Characterization of Bacterial Virulence Proteins. Cell Host Microbe. 2008;4: 8–15. doi:10.1016/j.chom.2008.06.004

57. Popa C, Coll NS, Valls M, Sessa G. Yeast as a Heterologous Model System to Uncover Type III Effector Function. Bliska JB, editor. PLOS Pathog. 2016;12: e1005360. doi:10.1371/journal.ppat.1005360

58. Robinson LA, Collins ACZ, Murphy RA, Davies JC, Allsopp LP. Diversity and prevalence of type VI secretion system effectors in clinical Pseudomonas aeruginosa isolates. Front Microbiol. 2023;13. doi:10.3389/fmicb.2022.1042505

59. Unterweger D, Miyata ST, Bachmann V, Brooks TM, Mullins T, Kostiuk B, et al. The Vibrio cholerae type VI secretion system employs diverse effector modules for intraspecific competition. Nat Commun. 2014;5: 3549. doi:10.1038/ncomms4549

60. Dar Y, Jana B, Bosis E, Salomon D. A binary effector module secreted by a type VI secretion system. EMBO Rep. 2022;23: e53981. doi:10.15252/embr.202153981

61. Wang W, Tang K, Wang P, Zeng Z, Xu T, Zhan W, et al. The coral pathogen Vibrio coralliilyticus kills non-pathogenic holobiont competitors by triggering prophage induction. Nat Ecol Evol 2022 68. 2022;6: 1132–1144. doi:10.1038/s41559-022-01795-y

62. Dunn AK, Millikan DS, Adin DM, Bose JL, Stabb E V. New *rfp*- and pES213-derived tools

for analyzing symbiotic *Vibrio fischeri* reveal patterns of infection and *lux* expression in situ. Appl Environ Microbiol. 2006;72: 802–810. doi:10.1128/AEM.72.1.802-810.2006

63. Gibson DG, Young L, Chuang RY, Venter JC, Hutchison CA, Smith HO. Enzymatic assembly of DNA molecules up to several hundred kilobases. Nat Methods. 2009;6: 343–345. doi:10.1038/nmeth.1318

64. Salomon D, Sessa G. Identification of growth inhibition phenotypes induced by expression of bacterial type III effectors in yeast. J Vis Exp. 2010; 4–7. doi:10.3791/1865

65. Bensadoun A, Weinstein D. Assay of proteins in the presence of interfering materials. Anal Biochem. 1976;70: 241–250. doi:10.1016/S0003-2697(76)80064-4

66. Li P, Kinch LN, Ray A, Dalia AB, Cong Q, Nunan LM, et al. Acute hepatopancreatic necrosis disease-causing Vibrio parahaemolyticus strains maintain an antibacterial type VI secretion system with versatile effector repertoires. Appl Environ Microbiol. 2017;83: e00737-17. doi:10.1128/AEM.00737-17

67. Cox J, Hein MY, Luber CA, Paron I, Nagaraj N, Mann M. Accurate proteome-wide label-free quantification by delayed normalization and maximal peptide ratio extraction, termed MaxLFQ. Mol Cell Proteomics. 2014;13. doi:10.1074/mcp.M113.031591

68. Tyanova S, Temu T, Sinitcyn P, Carlson A, Hein MY, Geiger T, et al. The Perseus computational platform for comprehensive analysis of (prote)omics data. Nature Methods. 2016. doi:10.1038/nmeth.3901

69. Perez-Riverol Y, Bai J, Bandla C, García-Seisdedos D, Hewapathirana S, Kamatchinathan S, et al. The PRIDE database resources in 2022: A hub for mass spectrometry-based proteomics evidences. Nucleic Acids Res. 2022;50. doi:10.1093/nar/gkab1038

70. Erlich Z, Shlomovitz I, Edry-Botzer L, Cohen H, Frank D, Wang H, et al. Macrophages, rather than DCs, are responsible for inflammasome activity in the GM-CSF BMDC model. Nature Immunology. 2019. doi:10.1038/s41590-019-0313-5

71. Lee I, Ouk Kim Y, Park S-C, Chun J. OrthoANI: An improved algorithm and software for calculating average nucleotide identity. Int J Syst Evol Microbiol. 2016;66: 1100–1103. doi:10.1099/ijsem.0.000760

72. Fridman CM, Keppel K, Gerlic M, Bosis E, Salomon D. A comparative genomics methodology reveals a widespread family of membrane-disrupting T6SS effectors. Nat Commun. 2020;11: 1085. doi:10.1038/s41467-020-14951-4

73. Jana B, Fridman CM, Bosis E, Salomon D. A modular effector with a DNase domain and a marker for T6SS substrates. Nat Commun. 2019;10: 3595. doi:10.1038/s41467-019-11546-6

74. Katoh K, Misawa K, Kuma K, Miyata T. MAFFT: a novel method for rapid multiple sequence alignment based on fast Fourier transform. Nucleic Acids Res. 2002;30: 3059–66. Available: http://www.ncbi.nlm.nih.gov/pubmed/12136088

75. Katoh K, Rozewicki J, Yamada KD. MAFFT online service: Multiple sequence alignment, interactive sequence choice and visualization. Brief Bioinform. 2018;20: 1160–1166. doi:10.1093/bib/bbx108

76. Saitou N, Nei M. The neighbor-joining method: a new method for reconstructing phylogenetic trees. Mol Biol Evol. 1987;4: 406–425. doi:10.1093/oxfordjournals.molbev.a040454